Supplementary Information

Dicarboxylate mediated efficient morphology/phase tailoring of $YPO_4:Ln^{3+}$ crystals and investigation of down-/up-conversion luminescence

Zhihao Wang,[a,b,c] Ji-Guang Li,[*a,b,c,] Qi Zhu,[a,b] Byung-Nam Kim,[c] Xudong Sun[a,b,d]

[a] Key Laboratory for Anisotropy and Texture of Materials, Northeastern University, Shenyang, Liaoning 110819, China

[b] Institute for Ceramics and Powder Metallurgy, School of Materials Science and Engineering, Northeastern University, Shenyang, Liaoning 110819, China

[c] Research Center for Functional Materials, National Institute for Materials Science, Namiki 1-1, Tsukuba, Ibaraki 305-0044, Japan

[d] School of Environmental and Chemical Engineering, Dalian University, Dalian, Liaoning 116622, China

*Corresponding author

Dr. Ji-Guang Li

National Institute for Materials Science

Tel: +81-29-860-4394

E-mail: Li.Jiguang@nims.go.jp

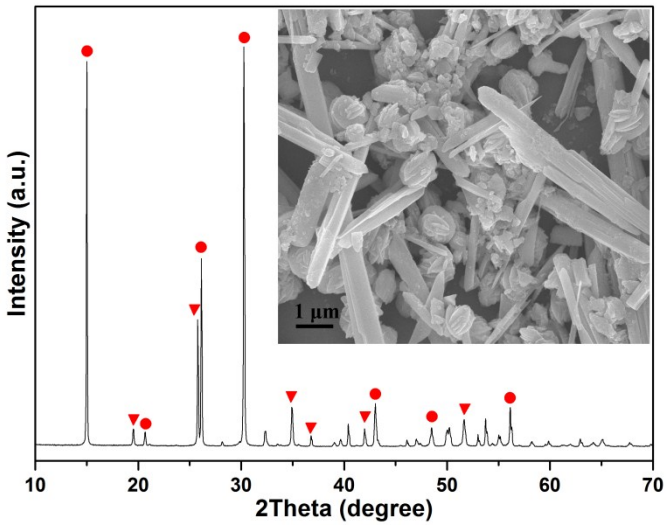

Fig. S1 XRD pattern and SEM image (the inset) of the comparative sample of S7. The red circles and triangles denote the hexagonal and tetragonal phases, respectively.

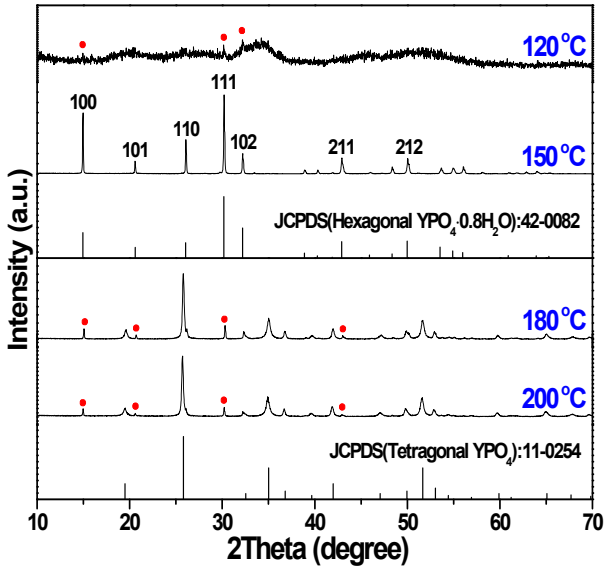

Fig. S2 XRD patterns for the products synthesized with the same experimental parameters of sample S4 but at the different hydrothermal temperatures indicated in the figure. The red circles denote the hexagonal phase.

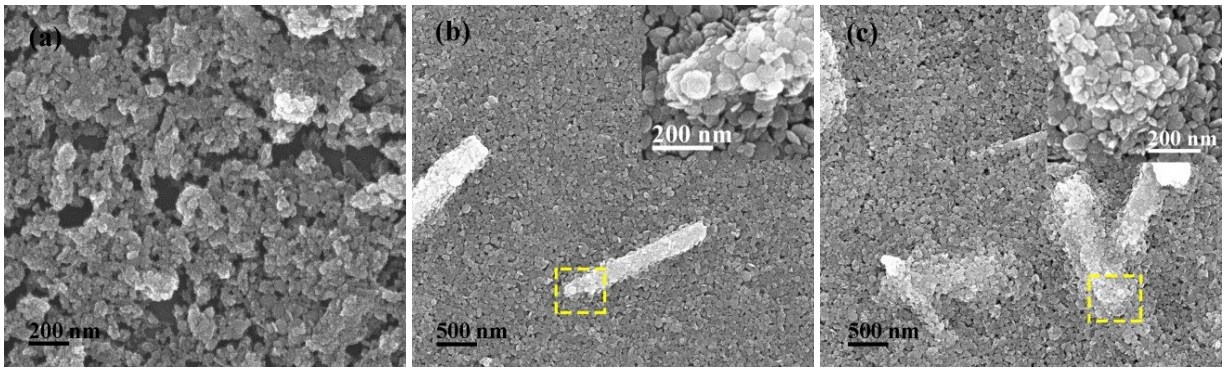

Fig. S3 SEM images of the products synthesized with the same experimental parameters as sample S4 but at the different hydrothermal temperatures of 120 °C (a), 180 °C (b) and 200 °C (c), respectively. The insets in (b) and (c) are the enlarged views of the corresponding rectangle regions.

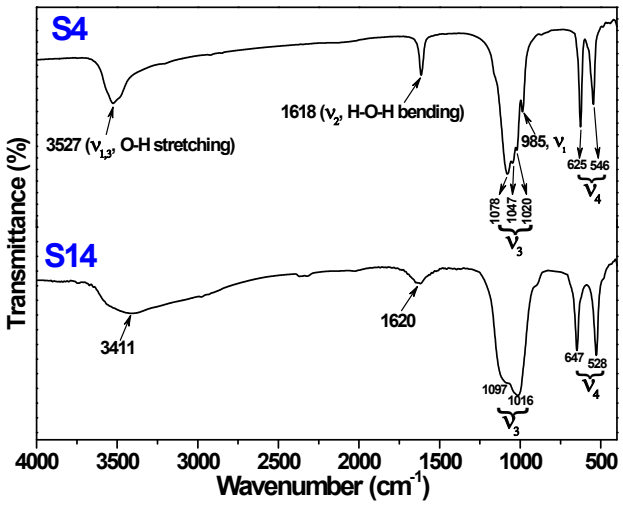

Fig. S4 FT-IR spectra for the h-$YPO_4 \cdot nH_2O$ (S4) and t-YPO_4 (S14) crystals

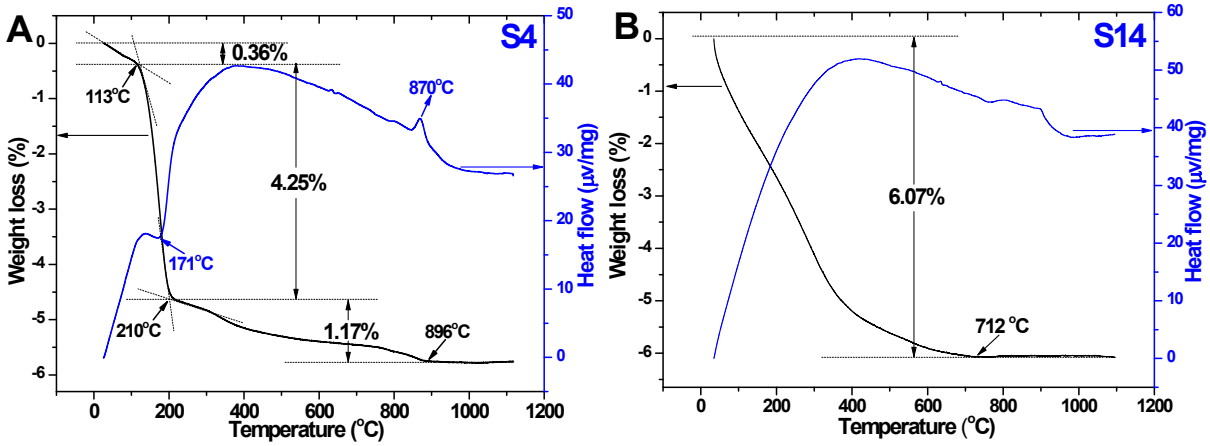

Fig. S5 TG/DTA profiles for S4 (A) and S14 (B).

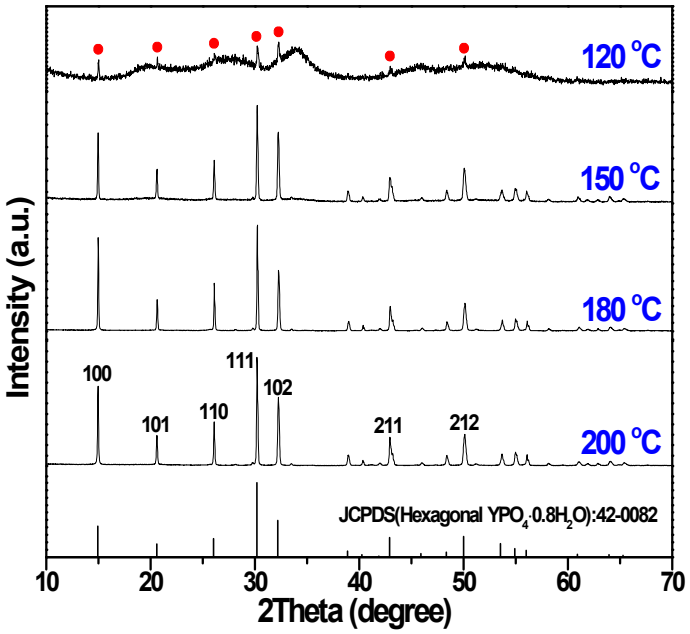

Fig. S6 XRD patterns of the products synthesized with the assistance of malate (Mal^{2-}:PO_4^{3-}:Y^{3+}=3:1:1) at pH=6 and the different hydrothermal temperatures indicated in the figure.

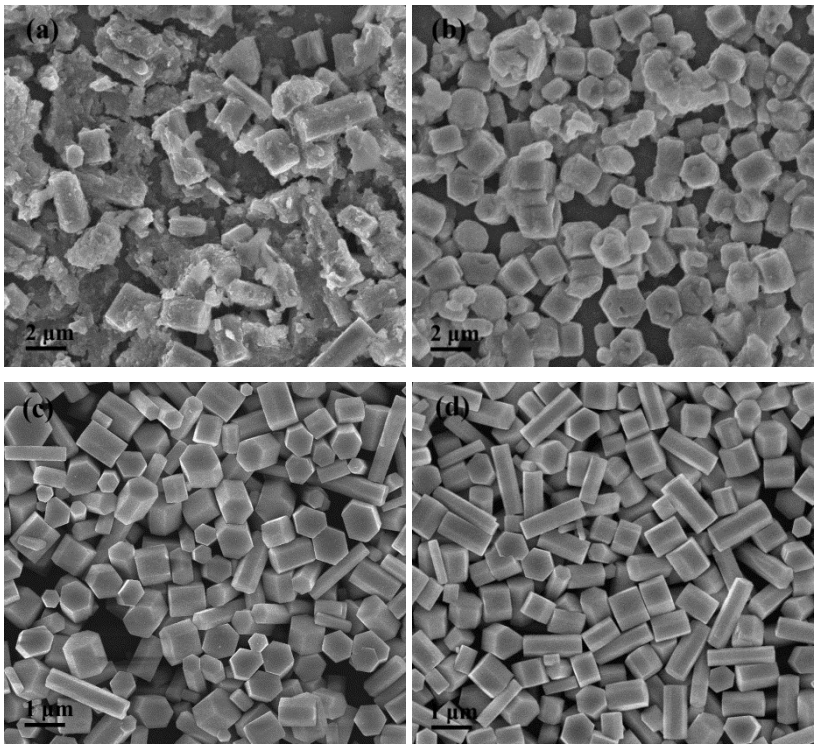

Fig. S7 SEM images of the products synthesized with the assistance of malate (Mal^{2-}:PO_4^{3-}:Y^{3+}=3:1:1) at pH=6 and the hydrothermal temperatures of 120 °C (a), 150 °C (b), 180 °C (c) and 200 °C (d).

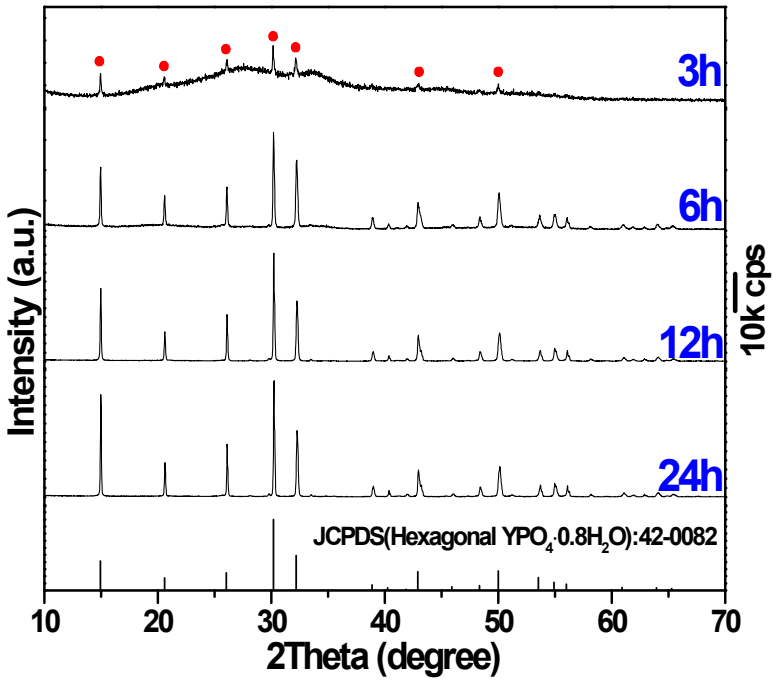

Fig. S8 XRD patterns for the samples synthesized with the assistance of malate (Mal^{2-}:PO_4^{3-}:Y^{3+}=3:1:1) at pH=6 and 180 °C. The reaction times are indicated in the figure.

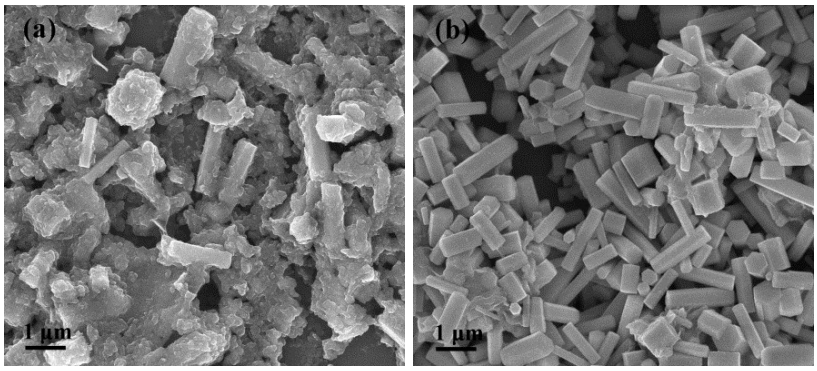

Fig. S9 FE-SEM images showing morphologies of the Mal^{2-}-assisted products, with the reaction time being 3h (a) and 6h (b).

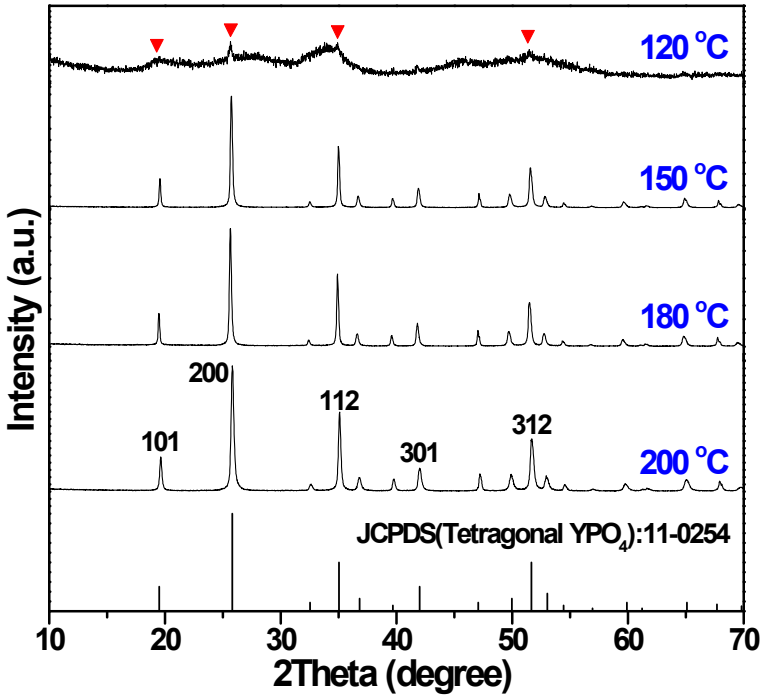

Fig. S10 XRD patterns of the products synthesized with the assistance of succinate (Suc^{2-}:PO_4^{3-}:Y^{3+}=3:1:1) at pH=6 and the hydrothermal temperatures indicated in the figure.

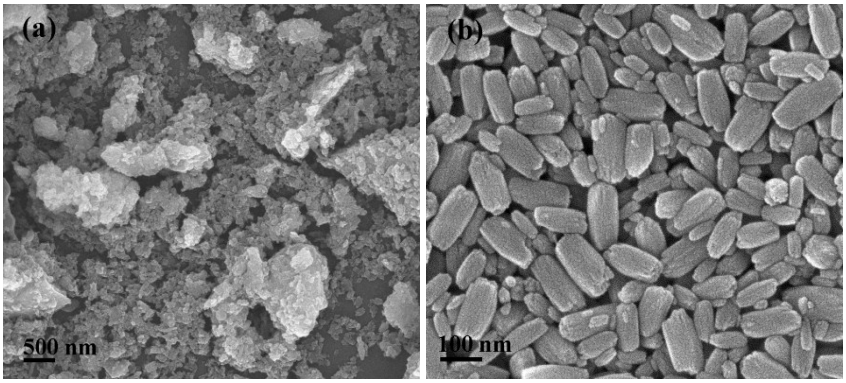

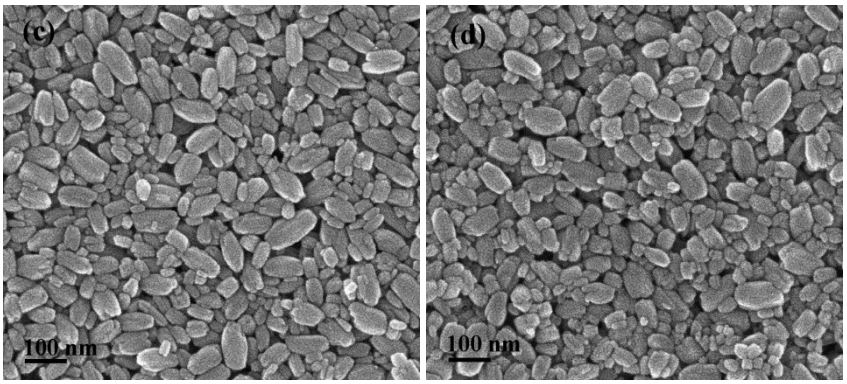

Fig. S11 SEM images of the products synthesized with the assistance of succinate (Suc^{2-}:PO_4^{3-}:Y^{3+}=3:1:1) at pH=6 and the hydrothermal temperatures of 120 °C (a), 150 °C (b), 180 °C (c), and 200 °C (d).

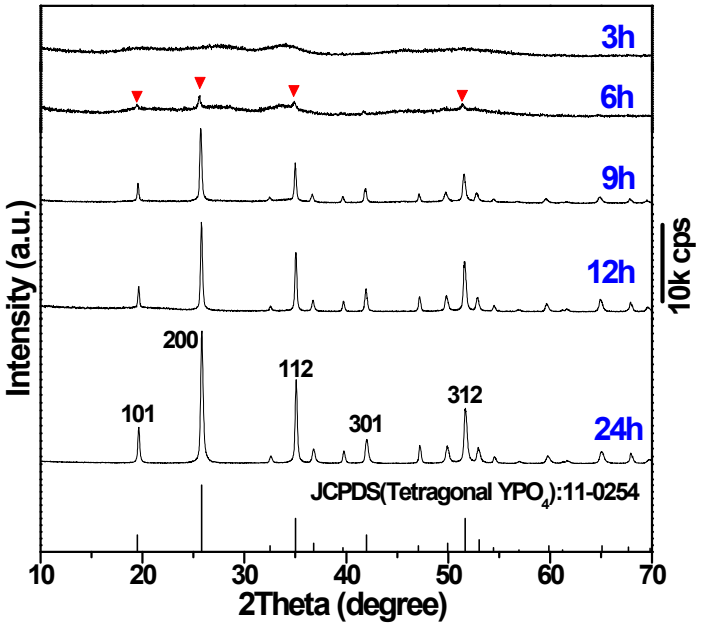

Fig. S12 XRD patterns for the samples synthesized with the assistance of succinate (Suc^{2-}:PO_4^{3-}:Y^{3+}=3:1:1) at 150 °C, with the reaction time indicated in the figure.

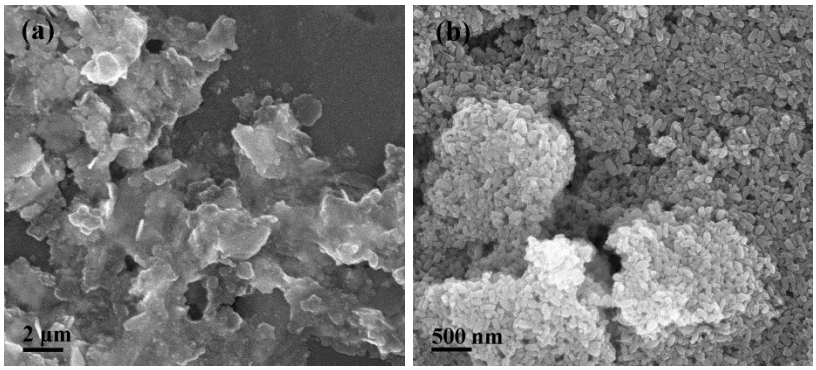

Fig. S13 FE-SEM images showing morphologies of the Suc^{2-} assisted products, with the reaction times being 6h (a) and 12h (b).

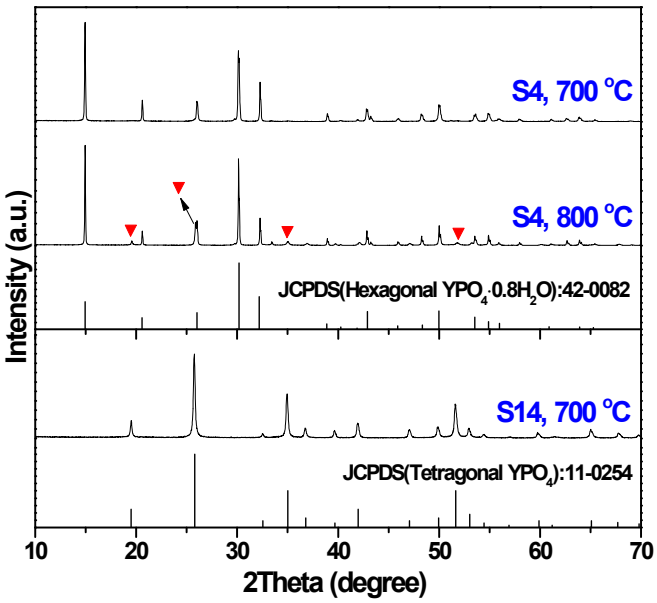

Fig. 14 XRD patterns of the products calcined from S4 at 700 and 800 °C and from S14 at 700 °C.

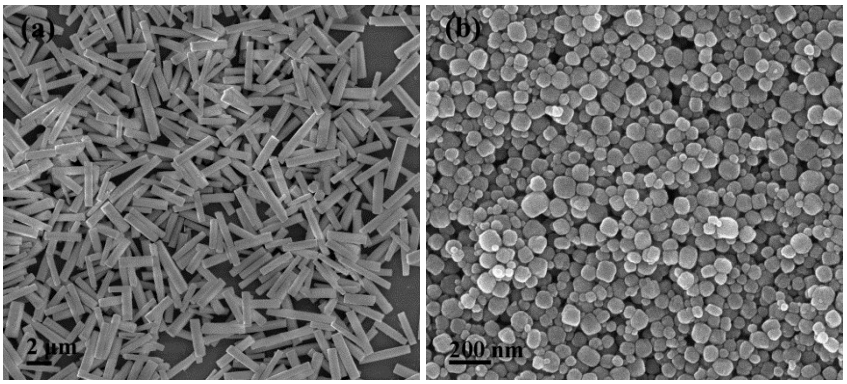

Fig. S15 SEM images showing morphologies of the products calcined from S4 (a) and S14 (b) at 700 °C.

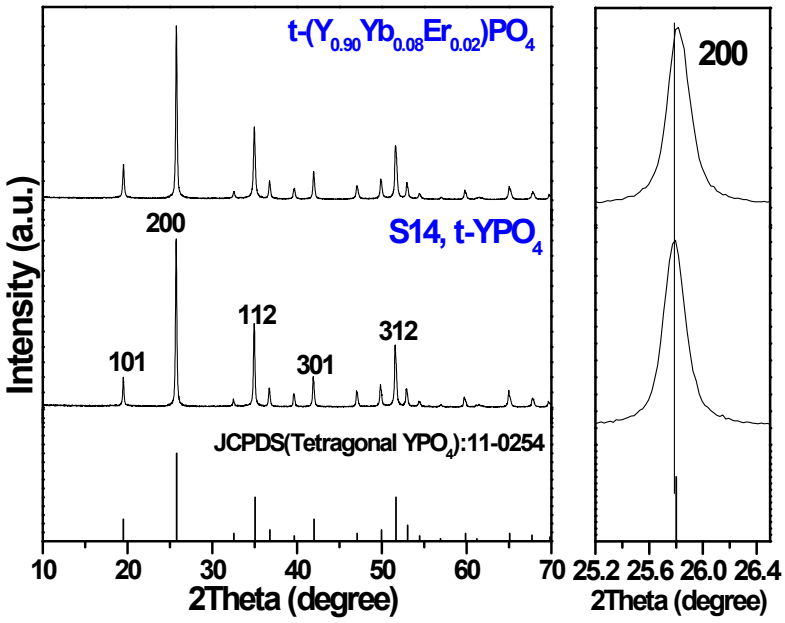

Fig. S16 XRD patterns of the t-$(Y_{0.90}Yb_{0.08}Er_{0.02})PO_4$ synthesized *via* hydrothermal reaction under the experimental conditions of sample S14, the right part is an enlarged view of the (200) diffraction region to show peak shifting.